

Multivalent linkers mediated ultra-sensitive bio-detection

Xiuyang Xia,^{1,2,*} Yuhan Peng,^{1,*} and Ran Ni^{1,†}

¹ School of Chemistry, Chemical Engineering and Biotechnology,
Nanyang Technological University, 62 Nanyang Drive, 637459, Singapore

² Arnold Sommerfeld Center for Theoretical Physics and Center for NanoScience,
Department of Physics, Ludwig-Maximilians-Universität München,
Theresienstraße 37, D-80333 München, Germany

In biosensing and diagnostic applications, a key objective is to design detection systems capable of identifying targets at very low concentrations, i.e., achieving high sensitivity. Here, we propose a linker-mediated detection scheme in which the presence of target molecules (linkers) facilitates the adsorption of ligand-coated guest nanoparticles onto a receptor-coated host substrate. Through a combination of computer simulations and mean-field theory, we demonstrate that, at fixed overall binding strength, increasing the valency of linkers exponentially lowers the concentration threshold for detection. This enables the identification of targets at extremely low concentrations, which is critical for early-stage disease and pathogen diagnostics. Furthermore, superselectivity with respect to binding strength is preserved for multivalent linkers, allowing for effective discrimination between targets and non-targets. Our findings highlight multivalency engineering of linkers as a powerful strategy to dramatically enhance the sensitivity of biodetection systems.

Introduction Biomarker and pathogen detection are pivotal for early disease diagnosis and personalized medicine [1, 2]. Conventional detection techniques, such as enzyme-linked immunosorbent assays (ELISA) [3] and polymerase chain reaction (PCR) [4], face inherent limitations, including high costs and the need for complex sample preparation [5, 6]. Moreover, achieving highly sensitive, superselective, and rapid detection remains a major challenge, particularly in complex biological matrices where biomarkers are often present at very low concentrations [7].

One promising solution to these challenges lies in the use of multivalency [8, 9]. Multivalent interactions occur when a single detection probe binds to multiple target sites, enhancing both the sensitivity and specificity of detection [10–14]. Previous studies have primarily focused on guest particle multivalency, where multivalent probes directly adsorb onto host substrates. Martinez-Veracoechea and Frenkel introduced the concept of superselectivity by investigating how multivalent guest particles bind to receptor-coated surfaces, demonstrating that adsorption can become highly sensitive to receptor density [11]. Moreover, by exploiting linker-mediated multivalent binding, detection systems can target biomarkers through sandwich-like architectures, even in the presence of competing molecules [15–21]. Recent experiments have shown that multivalent DNA-functionalized colloids can cooperatively bind to multiple repeated sequences in bacterial genomes, significantly improving detection sensitivity without the need for nucleic acid amplification [22]. However, the design principle underlying such sandwich-like systems with multivalent linkers (biomarkers) remains unclear. Specifically, how many binding sites on a linker are required to achieve sufficient sensitivity? While multivalency of linkers can enhance sensitivity, does it compromise the selectivity of the bind-

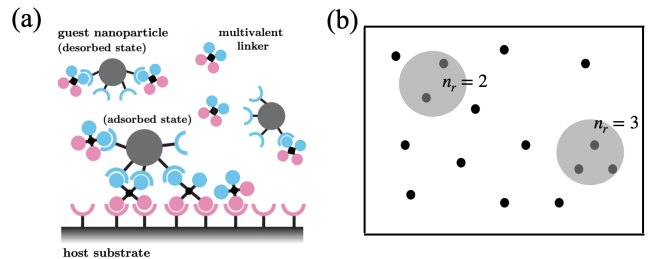


FIG. 1: **Multivalent linker-mediated adsorption of guest particles.** (a) Schematic illustration of the multivalent linker-mediated interaction between guest nanoparticles and the host substrate. Guest particles that form bridges to the substrate via linkers are considered in the adsorbed state, while those without such bridges are in the desorbed state. (b) Schematic of the GCMC simulation setup. Black dots represent immobile receptors randomly distributed on the substrate. Large gray circles indicate guest particles, each of which can interact only with receptors located within its own shaded region via linkers.

ing energy? Here, we combine the theoretical framework on multivalent linker-mediated interactions [23] and the Langmuir-like adsorption model [11] to design biodetection systems that achieve both ultra-sensitivity and superselectivity.

Method We consider a coarse-grained model in which guest particles adsorb onto a host substrate via multivalent linkers in the solution (Fig. 1a). These linkers can bind to multiple ligands on the guest particles and receptors on the host substrate. Following a Langmuir-like framework [23], we consider a substrate site with n_r immobile receptors that can accommodate at most one guest particle. Thus, each site exists either in a *desorbed* state, where no linker bridge is formed, or in an *adsorbed* state, where at least one linker bridges between the guest

particle and receptors on the substrate. A guest particle is coated with n_l mobile ligands, where the mobility of ligands allows them to potentially bridge with any receptor at its corresponding site, which ensures the validity of the combinatorial entropy term in our approximation. Linkers are treated as an ideal gas of density $\rho = e^{\beta\mu}/\Lambda^3$, with the chemical potential μ , de Broglie wavelength Λ , and the inverse thermal energy $\beta = 1/k_B T$, where k_B and T are the Boltzmann constant and system temperature, respectively. Each linker possesses κ_l and κ_r binding ends for ligands on guest particles and the receptors on substrate, with individual binding free energies f_l and f_r , respectively.

We formulate the grand potential of the system in both desorbed and adsorbed states. Our approach follows Ref. [23] and has been validated by thermodynamic integration for systems with explicit multivalent linkers. The central idea is to treat each linker as interacting only with receptors on a single substrate site and ligands on the associated guest particle, assuming that the linker size is small compared to the site and guest particles. Thus, linkers mediate an effective interaction between the substrate and the guest particle, without coupling with other sites. In the adsorbed state, aside from the free linkers in solution, each linker can be dangling from receptors on the substrate site, dangling from ligands on the guest particle, or bridging between receptors and ligands, thereby connecting the site and the particle. For each of these possibilities, we further enumerate substates corresponding to the specific number of bonds formed by each linker. Then, we derive the grand partition function for linkers in each substate, taking into account all possible binding combinations and the indistinguishability of bonds. By applying the saddle-point approximation, we determine the equilibrium number of linkers in each state: M_l for those dangling on ligands, M_r for those dangling on receptors, and Q for those that form bridges (see SI Sec. I). The resulting grand potential for the adsorbed state is

$$\beta F_{\text{ad}} = \sum_{i \in \{l, r\}} (n_i \log \bar{n}_i - \bar{n}_i - M_i) + Q, \quad (1)$$

where \bar{n}_i denotes the number of unbound ligands ($i=l$) or receptors ($i=r$) in the adsorbed state. Similarly, for the desorbed state, only dangling linkers exist, as no bridges can form when the guest particle is far from the site. The grand-canonical potential in the desorbed state is given by

$$\beta F_{\text{de}} = \sum_{i \in \{l, r\}} (n_i \log \bar{n}'_i - \bar{n}'_i - M'_i), \quad (2)$$

where M'_l and M'_r represent the numbers of linkers dangling from ligands and receptors, respectively, and \bar{n}'_i represents the number of unbound ligands or receptors when the guest particle is infinitely far from the site. All M ,

Q , and \bar{n} are numerically calculated by solving a set of self-consistent equations, in which the convergence of the solution for arbitrary linker valency is ensured [23].

We assume that adsorption events on individual substrate sites are independent, with no interactions between particles adsorbed on adjacent sites. For each site, we take the desorbed state as the reference, and define the partition function of the adsorbed state as $q = e^{-\beta(F_{\text{ad}} - F_{\text{de}})} - 1$ [13]. The grand partition function, averaged over all substrate sites, is then given by $\Xi = \langle 1 + z_g q \rangle_{\langle n_r \rangle}$, where z_g is the activity of guest nanoparticles in the bulk solution, proportional to the particle density and adsorption volume [11, 21]. $\langle \cdot \rangle_{\langle n_r \rangle}$ calculates the average over the Poisson distribution of uncorrelated, immobile receptors, characterized by the mean $\langle n_r \rangle$. The probability of nanoparticle adsorption follows a Langmuir-type isotherm:

$$\theta := \frac{\partial \log \Xi}{\partial \log z_g} = \left\langle \frac{z_g q}{1 + z_g q} \right\rangle_{\langle n_r \rangle}. \quad (3)$$

To validate our theoretical prediction and provide a parameter mapping for future studies, we performed Grand Canonical Monte Carlo (GCMC) simulations of a monolayer of guest nanoparticles in contact with host substrate coated with explicit receptors. Guest particles are modeled as hard disks with diameter $\sigma = 1$ on a two-dimensional substrate, and are in chemical equilibrium with a reservoir of guest nanoparticles at chemical potential μ_g above the substrate [21] (see Fig. 1b). The activity of guest particles is given by $z_g = e^{\beta\mu_g} \pi \sigma^2 h_0 / (4\Lambda^3)$, where $h_0 = 1$ is the thickness of the adsorption layer. Immobile receptors are randomly distributed on the substrate following a Poisson distribution with number density ρ_r . Mobile ligands on each guest particle can interact with receptors located within the area underneath the nanoparticle. Guest particles are allowed to move freely on a two-dimensional plane of box length L with periodic boundary conditions. The maximum number of adsorption sites in the simulation is set to $N_{\text{max}} = 4L^2 / (\pi\sigma^2)$. The adsorption probability θ is calculated as $\langle N_g \rangle / N_{\text{max}}$, where $\langle N_g \rangle$ is the average number of guest particles adsorbed on the plane.

We focus on how linker multivalency, and the corresponding additional combinatorial entropy, modulate two key features of multivalent adsorption systems: sensitivity and selectivity. Here, sensitivity refers to the lowest detectable value of a given environmental parameter χ^* at which adsorption becomes significant. Operationally, we define the sensitivity threshold χ^* by the condition $\theta(\chi^*) = 0.1$. Selectivity quantifies the degree to which adsorption responds to changes in χ , and is characterized by the selectivity parameter $\alpha_\chi = d \log \theta / d \log \chi$. When $\alpha_\chi > 1$, the adsorption increases superlinearly with respect to the environmental parameter, $\theta \sim \chi^{\alpha_\chi}$. Conversely, $\alpha_\chi < -1$ indicates that the nanoparticle desorption also proceeds in a superlinear fashion. Both regimes

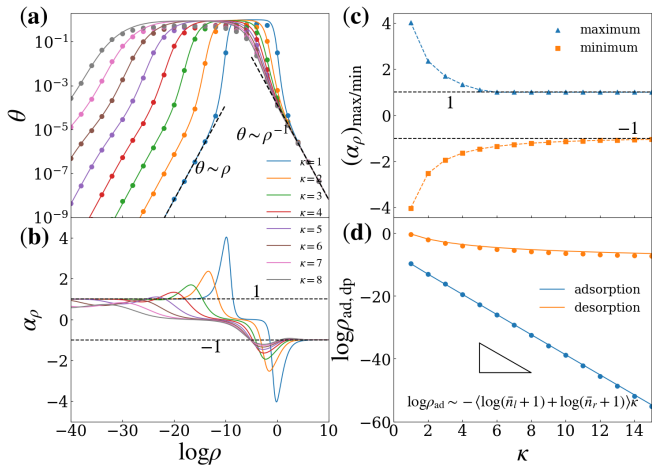


FIG. 2: ρ -dependent superselectivity and ultrasensitivity. Here, $\kappa\beta f_l = \kappa\beta f_r = -5$, $n_l = \langle n_r \rangle = 10$, $\beta f_{\text{conf}} = 2$, and $z_g = 10^{-5}$. The dot symbols are simulation results, and the solid curves are the theoretical results. (a) The adsorption probability θ as a function of $\log \rho$ under different valencies of linkers. The dashed lines indicate the low-concentration and high-concentration limits of θ . (b) The selectivity α_ρ to linker concentration as a function of $\log \rho$ under different valencies. (c) The maximal and minimal selectivity $(\alpha_\rho)_{\max/\min}$ as a function of linker valency κ . The colored dashed lines are merely guides for the eyes. The dashed lines are guides of eyes where the curves converge to (d) Log of the adsorption and desorption sensitivity thresholds $\log \rho_{\text{ad,dp}}$ as a function of linker valency κ . The small triangle gives the converging slope of the desorption curve.

are referred to as χ -dependent superselectivity. Superselectivity endows the system with highly specific discrimination between target and non-target conditions, facilitating the exclusion of non-target components or background noise. For example, achieving superselectivity with respect to the bridge energy enables the system to respond almost exclusively to target molecules with the desired binding characteristics, minimizing false positives from background species.

Ultrasensitive ρ -response To investigate the influence of linker valency κ on adsorption behavior and selectivity, we perform both theoretical analysis and GCMC simulations, with $\kappa = \kappa_l = \kappa_r$. In all calculations, we fix the overall bridging strength at $f = \kappa f_l = \kappa f_r$, so that an increase in κ corresponds to a decrease in the individual binding strength $\beta f_{l/r}$. This allows us to isolate the effect of linker valency by eliminating changes in overall binding strength, ensuring that any observed variation in adsorption behavior arises solely from the combinatorial entropy introduced by varying multivalency.

Figure 2 systematically illustrates how linker multivalency shapes both the adsorption profile and selectivity with respect to linker concentration ρ . As shown in Fig. 2a, the adsorption probability θ increases linearly with ρ at low concentrations, followed by a pro-

nounced nonlinear regime. Remarkably, at high linker concentrations, after a saturation plateau, θ begins to decrease as ρ increases further, which is a distinct feature of linker-mediated interactions[24, 25]. The corresponding selectivity parameter α_ρ , shown in Fig. 2b, reveals that for moderate linker valency κ , both adsorption and desorption transitions are superselective with respect to ρ . Specifically, the maxima and minima of α_ρ exceed 1 in magnitude ($\alpha_{\rho,\max} > 1$, $\alpha_{\rho,\min} < -1$), signifying highly cooperative, superlinear responses as the system transitions between desorbed and adsorbed states. Interestingly, as κ increases, the selectivity weakens: $\alpha_{\rho,\max}$ decreases and $\alpha_{\rho,\min}$ increases, both approaching 1 and -1 in the large valency limit (see Fig.2c). This trend is rooted in the combinatorial nature of multivalency. In the limit of vanishing guest particle activity $z_g \rightarrow 0$ and strong individual binding $f_{l/r} \rightarrow -\infty$, our mean-field analysis predicts that the maximal selectivity decays as $\alpha_{\rho,\max} \approx \min(n_l, n_r)/\kappa$ (see SI Sec.III.D), indicating that the number of bridges ultimately limits the attainable superselectivity. When κ exceeds $\min(n_l, n_r)$, the system loses its superselective response to linker concentration. In realistic regimes of finite $f_{l/r}$ and z_g , the selectivity is reduced even further, consistent with MC simulation results.

In addition to selectivity, linker valency also strongly affects the adsorption and desorption sensitivity thresholds ρ_{ad} and ρ_{dp} . Figure 2d shows that ρ_{ad} decreases exponentially with increasing κ , while ρ_{dp} decreases and then plateaus at large κ . The relationship between θ and the effective interaction free energy F_{eff} is direct, but the dependence of F_{eff} on ρ is more subtle, as it reflects the underlying combinatorial entropy of multivalent binding. We first analyze how F_{eff} determines the critical linker concentration at the adsorption sensitivity threshold ρ_{ad} . To this end, we first focus on a substrate site with n_l ligands and n_r receptors, temporarily neglecting the distribution of receptor numbers. In the large- κ limit, both adsorbed and bridged linkers become extremely sparse, as only a very small number of linkers are required to fully bind the guest particle (or its corresponding adsorption site). Consequently, the M and Q terms in Eq. 1 can be neglected. Meanwhile, the absolute free energy in the desorbed state is negligible ($F_{\text{dp}} \approx 0$), due to the greatly reduced combinatorial entropy in this regime. Under these conditions, the effective interaction between a guest particle and its substrate site can be simplified as

$$\beta F_{\text{eff}} \simeq \sum_{i=l,r} \left[n_i \log \left(\frac{\bar{n}_i}{n_i} \right) - (\bar{n}_i - n_i) \right], \quad (4)$$

where \bar{n}_i ($i=l,r$) denotes the number of unbound ligands or receptors in the adsorbed state at $\theta(\chi^*)=0.1$ (see SI Sec. III.E). In the large-valency regime, and under the Poisson distribution of receptor numbers, this yields

$$\log \rho_{\text{ad}} \sim - \lim_{\kappa, n_r \rightarrow \infty} [\log(\bar{n}_l + 1) + \log(\bar{n}_r + 1)] \kappa. \quad (5)$$

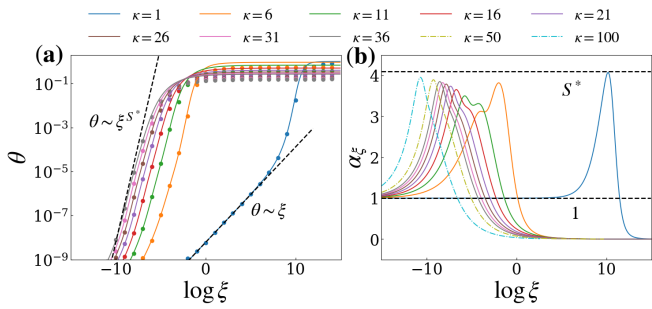


FIG. 3: ξ -dependent superselectivity. Here, $\log \rho = -10$, $n_l = \langle n_r \rangle = 10$, $\beta f_{cnf} = 2$, $z_g = 10^{-5}$, and $S^* = \lim_{\kappa \rightarrow \infty} \kappa \bar{n} \sqrt{\xi}$. The dots represent simulation results, while the solid lines indicate the theoretical results. (a) The adsorption probability θ as a function of $\log \xi$, where $\xi = e^{-\beta f} = e^{-\beta f_l - \beta f_r}$. The dashed line $\theta \sim e^{-\beta f}$ gives the behavior under low binding strength limit, while the other dashed line $\theta \sim e^{-S^* \beta f}$ gives the superselectivity at large valency limit. (b) The selectivity with respect to the binding partition function ξ as a function of binding strength $\log \xi$. The upper dashed lines indicate the lower boundary of the superselectivity at the large valency limit. The lower dashed line is a guide for the eyes for selectivity at the low binding strength limit.

This shows that the critical linker concentration for the onset of adsorption, ρ_{ad} , decreases exponentially with increasing linker valency κ , with the exponent given by $-\lim_{\kappa, n_r \rightarrow \infty} [\log(\bar{n}_l + 1) + \log(\bar{n}_r + 1)]$. As the total binding strength $\kappa f_{l,r}$ is fixed, this exponential scaling reflects the dominant contribution of the combinatorial entropy associated with linker multivalency. This intriguing result suggests that even with a fixed overall binding strength, i.e., $f = \kappa f_l = \kappa f_r$, increasing κ can exponentially lower the adsorption threshold or detection limit, thereby enabling ultrasensitive detection.

In contrast, the desorption threshold ρ_{de} approaches a constant as κ increases (Fig. 2d). This convergence appears because, with increasing κ , the enhanced combinatorial entropy strongly favors a fully bound state between ligands on the nanoparticle and receptors on the substrate. As a result, further increasing κ does not increase the number of bound ends per linker, and the effective interaction, along with the corresponding ρ_{de} , becomes purely entropically driven and saturates in the large- κ limit. This behavior is qualitatively consistent with the purely entropy-driven phase behavior observed in programmable colloidal atom-electron equivalents at large linker valency [23].

Superselective ξ -response Next, we investigate whether multivalent linker-mediated binding can exhibit superselectivity with respect to the binding strength, a property that is crucial for suppressing nonspecific interactions in complex biomolecular environments. For simplicity, we first consider the symmetric case $f_l = f_r = \beta f / 2$ and $n_l = n_r$, but the essential physics and analysis can be readily generalized to asymmetric

systems with $\kappa_l \neq \kappa_r$ or $n_l \neq n_r$ (see SI Sec. V). Figure 3a shows the adsorption probability as a function of the binding strength parameter $\xi = \exp(-\beta f)$. As κ increases, the adsorption curve shifts towards weaker binding strengths. In the low linker valency regime, this shift is primarily due to the increase in total binding strength as valency increases. Whereas, in the large valency regime, the shift is dominated by the enhanced combinatorial entropy, which allows ligands and receptors to be fully bound even at weaker binding strengths.

Distinct from the case of linker concentration, the maximum selectivity with respect to binding strength, quantified by $\alpha_{\xi, \max}$, remains above 1 even at large κ , indicating persistent superselectivity. As shown in Fig. 3b, the selectivity parameter α_ξ shows a single peak for bivalent systems ($\kappa = 1$). However, interestingly, in multivalent systems, a second peak emerges at lower binding strength, while the original peak at higher binding strength gradually diminishes with increasing κ . Notably, the maximum selectivity $\alpha_{\xi, \max}$ converges to a finite value as κ increases. These two peaks arise from different mechanisms. The peak at higher ξ originates from the multivalency of the guest particles themselves, as previously described [11, 21]; here, the superselective response results from the nonlinear formation of bridges between guest particles and the substrate. In contrast, the newly emerging peak at low ξ is primarily driven by linker multivalency itself. As the binding strength increases, each linker forms more bonds with ligands and receptors, but the number of fully bridged linkers grows much more slowly. Thus, the sharp increase in selectivity can be attributed mainly to the rapid growth in the number of bonds on linkers. The position of this new peak approximately corresponds to the point where the average number of bonds per linker increases most rapidly.

Using mean-field theory, we estimate the lower bound of the converged selectivity peak, which becomes exact in the low linker concentration limit. At large valency and low concentration, the average number of bonds formed between a linker and a guest particle (or the substrate) simplifies to (see SI Sec. V)

$$\kappa_{\text{link}} \approx 2\kappa \bar{n} \sqrt{\xi}, \quad (6)$$

where \bar{n} is the number of unbound ligands or receptors. In this regime, superselectivity arising from linker multivalency appears when most ligands or receptors remain unbound ($\bar{n} \rightarrow n$). By approximating the first-order solution of the self-consistent equation, the selectivity at the peak can be expressed as (see SI Sec. V)

$$\alpha_{\xi, \max} \approx \kappa \bar{n} \sqrt{\xi} \approx \frac{\kappa_{\text{link}}}{2}. \quad (7)$$

In the large valency limit, $\kappa \bar{n} \sqrt{\xi} \rightarrow S^*$, where S^* is a constant. As the above approximations may underestimate

the true peak, S^* serves as a lower bound for the converged selectivity.

Our theory thus demonstrates that superselectivity persists even at large κ , with the maximal selectivity determined by the number of ligands (or receptors), chemical potential, and configurational entropy penalty. Notably, lower linker concentration leads to even higher selectivity. This finding suggests that linker multivalency enables highly sensitive detection of target linkers at low concentrations, while minimizing nonspecific interactions with non-targeted linkers. For systems with a distribution of n_r , similar results are obtained (see SI Sec. V).

Conclusion In summary, we have established a theoretical framework for understanding how the multivalency of linkers controls the sensitivity and selectivity in bio-detection. Our results reveal that increasing linker valency dramatically enhances the sensitivity, enabling detection at ultralow concentrations through an exponential reduction of the adsorption threshold. This ultrasensitive effect implies that even a sparse concentration of multivalent linkers can trigger a strong binding signal, which is promising for detecting very sparse biomarkers or pathogens. This enhancement comes with a trade-off: large valency diminishes superselectivity with respect to linker concentration, making the adsorption response less discriminating as the linker number increases. However, importantly, we show that superselectivity with respect to binding strength persists even in the large valency regime, allowing robust discrimination between target and non-target species. Our results suggest that, in designing the detection system, it is not always optimal to select ligands and receptors that bind strongly to the target (linker); instead, those capable of binding to multiple sites on the target may be more effective. These findings provide general design principles for engineering multivalent detection systems and highlight the fundamental role of entropy in controlling biomolecular recognition. Our theory thus offers practical guidelines for developing next-generation biosensors and diagnostic assays capable of ultra-sensitive and highly specific detection in complex biological environments.

X. X. acknowledges support from the Alexander von Humboldt-Stiftung. This work was financially supported by the Academic Research Fund from the Singapore Ministry of Education (RG151/23, and RG88/25) and the National Research Foundation, Singapore, under its 29th Competitive Research Program (CRP) Call (NRF-CRP29-2022-0002).

[†] Electronic address: r.ni@ntu.edu.sg

- [1] L. M. Shaw, M. Korecka, C. M. Clark, V. M.-Y. Lee, and J. Q. Trojanowski, *Nature reviews Drug discovery* **6**, 295 (2007).
- [2] K. K. Jain and K. K. Jain, *Textbook of Personalized Medicine* pp. 103–113 (2021).
- [3] E. Engvall and P. Perlmann, *Immunochemistry* **8**, 871 (1971).
- [4] K. B. Mullis and F. A. Faloona, in *Methods in enzymology* (Elsevier, 1987), vol. 155, pp. 335–350.
- [5] S. Aydin, *Peptides* **72**, 4 (2015).
- [6] S. A. Bustin and T. Nolan, *Journal of biomolecular techniques: JBT* **15**, 155 (2004).
- [7] J. D. Wulfkuhle, L. A. Liotta, and E. F. Petricoin, *Nature Reviews Cancer* **3**, 267 (2003).
- [8] J. Huskens, *Curr. Opin. Chem. Biol.* **10**, 537 (2006).
- [9] P. I. Kitov and D. R. Bundle, *J. Am. Chem. Soc.* **125**, 16271 (2003).
- [10] D. Lukatsky and D. Frenkel, *Physical review letters* **92**, 068302 (2004).
- [11] F. J. Martinez-Veracoechea and D. Frenkel, *Proceedings of the National Academy of Sciences* **108**, 10963 (2011).
- [12] G. V. Dubacheva, T. Curk, R. Auzély-Velty, D. Frenkel, and R. P. Richter, *Proc. Natl. Acad. Sci. U.S.A.* **112**, 5579 (2015).
- [13] S. Angioletti-Uberti, *Physical Review Letters* **118**, 068001 (2017).
- [14] T. Curk, C. A. Brackley, J. D. Farrell, Z. Xing, D. Joshi, S. Direito, U. Bren, S. Angioletti-Uberti, J. Dobnikar, E. Eiser, et al., *Proceedings of the National Academy of Sciences* **117**, 8719 (2020).
- [15] T. A. Taton, C. A. Mirkin, and R. L. Letsinger, *Science* **289**, 1757 (2000).
- [16] Y. C. Cao, R. Jin, and C. A. Mirkin, *Science* **297**, 1536 (2002).
- [17] P. L. Biancaniello, A. J. Kim, and J. C. Crocker, *Physical review letters* **94**, 058302 (2005).
- [18] H. Xiong, D. van der Lelie, and O. Gang, *Phys. Rev. Lett.* **102**, 015504 (2009).
- [19] X. Xia, H. Hu, M. P. Ciamarra, and R. Ni, *Sci. Adv.* **6**, eaaz6921 (2020).
- [20] T. Curk, G. V. Dubacheva, A. R. Brisson, and R. P. Richter, *J. Am. Chem. Soc.* **144**, 17346 (2022).
- [21] X. Xia and R. Ni, *Physical Review Letters* **132**, 118202 (2024).
- [22] P. Xu, T. Cao, Q. Fan, X. Wang, F. Ye, and E. Eiser, *Proceedings of the National Academy of Sciences* **120**, e2305995120 (2023).
- [23] X. Xia, Y. Peng, K. Li, and R. Ni, *Rep. Prog. Phys.* **88**, 078101 (2025).
- [24] X. Xia, H. Hu, M. P. Ciamarra, and R. Ni, *Science Advances* **6**, eaaz6921 (2020).
- [25] J. Lowensohn, B. Oyarzún, G. Narváez Paliza, B. M. Mognetti, and W. B. Rogers, *Phys. Rev. X* **9**, 041054 (2019).

* These authors contributed equally.